Deep non-invasive Raman spectroscopy of living tissue and powders†

Pavel Matousek

Received 8th March 2007
First published as an Advance Article on the web 9th May 2007
DOI: 10.1039/b614777c

This *tutorial review* examines emerging Raman spectroscopy techniques for deep non-invasive probing of diffusely scattering media such as living tissue and powders. As generic analytical tools, the methods pave the way for a range of new applications for Raman spectroscopy, including disease diagnosis, non-invasive probing of pharmaceutical products in quality control and security screening.

1. Introduction

One of the most important goals of the analytical sciences in biomedical research is the provision of a highly chemically specific, non-invasive method for monitoring the composition of deep layers in turbid media such as living tissue. Such chemically specific information is important, for example, in medical diagnosis as diseases are often accompanied by biochemical changes. Other applications include the non-invasive probing of pharmaceutical products in quality control applications, drug authentication and security screening for the presence of harmful substances. Presently, the key optical spectroscopic techniques that are potentially applicable to these problems include near-infrared (NIR) absorption spectroscopy, mid-infrared (MIR) spectroscopy and Raman spectroscopy. Although NIR is widely used in a number of these areas, in many uses it suffers from limited chemical specificity.[1] Examples of the application areas not addressed effectively include the non-invasive diagnosis of osteoporosis and deeply buried breast cancer lesions, the non-invasive monitoring of glucose concentrations in blood *in vivo* and the non-invasive bulk monitoring of low concentration polymorphs in pharmaceutical applications. In comparison, both MIR and Raman spectroscopies offer a substantially higher degree of chemical specificity but, so far, their use has been confined mainly to applications involving only shallow layers of turbid media. In the case of MIR spectroscopy, the key reason for this is its incompatibility with aqueous samples, as water absorbs MIR radiation strongly, precluding deep probing of living tissue *in vivo* and examination of pharmaceutical products, *e.g.* aqueous slurries. From this perspective, Raman spectroscopy holds much greater promise as it does not suffer from the same problem; the Raman signal of water is very weak and water itself does not absorb the probe and Raman light. It should be noted that there are also other specialised techniques for probing turbid media, such as X-ray analysis, THz absorption spectroscopy, positron emission tomography (PET), nuclear magnetic resonance (NMR) spectroscopy, and ultrasound. Whilst some of these techniques are very potent and widely used in many key biomedical applications, they also possess some limitations; most notably, they are costly, involve ionising radiation and/or do not have adequate sensitivity for a range of diagnostic applications.

The Raman effect is the inelastic scattering of photons from molecules *via* interactions with the vibrational modes within the molecule. In this process, the photon energy and consequently the photon wavelength are altered.[1] This change gives a specific spectral signature unique to each chemical species undergoing the scattering (see Fig. 1). Most commonly, the photon loses energy and its wavelength is shifted, typically, by several hundreds to thousands of wavenumbers away from the laser wavelength, towards longer wavelengths. The Raman shift, or energy loss, is directly related to the frequency of vibrational motion activated within the molecule. As vibrational modes have frequencies that are highly specific to the chemical constitution of the molecule, the identity and structure of the molecule can be deduced.

The applicability of this technique is limited to samples that do not exhibit strong fluorescence emission in the spectral region coincident with the Raman spectra as this can easily swamp the relatively weak Raman signals.[1] The emission can,

Central Laser Facility, CCLRC Rutherford Appleton Laboratory, Didcot, Oxfordshire, UK OX11 0QX. E-mail: P.Matousek@rl.ac.uk; Fax: +44 (0)1235-445693; Tel: +44 (0)1235-445377

† The HTML version of this article has been enhanced with colour images.

Pavel Matousek

Pavel Matousek obtained his MSc and PhD degrees in physics from the Czech Technical University, Prague, the Czech Republic, the latter in partnership with the CCLRC Rutherford Appleton Laboratory (RAL), UK. From 1991, he has worked at the Central Laser Facility, RAL, where he is presently a Programme Manager at the Lasers for Science Facility. His research includes the use of steady-state and time-resolved Raman spectroscopy in the investigation of short lived intermediates, the rejection of fluorescence from Raman spectra and the application of nonlinear optics in spectroscopy and high power laser research. His current research focuses on the development of deep non-invasive Raman methods for biomedical and pharmaceutical applications.

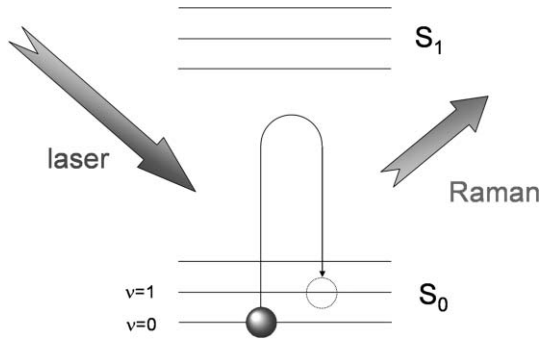

Fig. 1 Depiction of the molecular vibrational (ν) and electronic (S) energy levels involved in a typical Raman scattering process in the NIR spectral region.

for example, originate from the probed molecule or other constituents or impurities in the sample. Noise is present in the spectra due to the fact that fluorescence backgrounds, as well as the Raman signal itself, in general, follow Poisson statistics and contribute with inherent, irremovable photon shot noise. Its amplitude is proportional to the square root of the number of photons registered by the detector, often termed photoelectrons, at a given detection channel.[1] Consequently, even after the subtraction of a polynomial fluorescence background, the noise remains imprinted on the measured Raman spectra, thus reducing the signal-to-noise ratio of the ultimate Raman spectra or even overwhelming the Raman signal entirely. The fluorescence problem can be eliminated, or at least minimised, using near-infrared excitation away from the electronic absorption bands of most fluorescing species, thus preventing their excitation and the consequential generation of fluorescence emission.

To date, the Raman method has been used with modern Raman probes and microscopes predominantly in the backscattering collection mode (see Fig. 2), although some laboratory instruments designed for small volume samples use 90° collection geometry, where the laser is perpendicular to the Raman collection axis. The backscattering mode gained its popularity with Raman probes and microscopes for its instrumental simplicity and ease of use, often in conjunction with confocal microscopy permitting effective depth discrimination of Raman signals in transparent and semi-transparent media or in turbid (*i.e.* diffusely scattering) media at shallow depths where the medium still appears to be semi-transparent.[1] For example, in living tissue its penetration depth is typically only several hundred micrometres, leaving many tissue components, such as bones and deep cancerous tissue, inaccessible. With pharmaceutical products such as tablets, the accessible depth is somewhat larger, typically in the range of 1 mm, but this again is insufficient for probing the bulk composition of a typical pharmaceutical tablet.

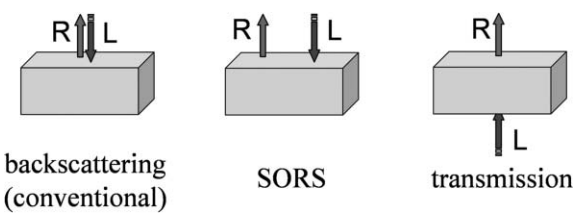

Fig. 2 Basic types of Raman spectroscopy geometries with respect to the sample. Left: conventional backscattering Raman; centre: SORS (spatially offset Raman spectroscopy, see below); and right: Raman transmission geometries. Legend: R: Raman light; L: laser beam.

A substantial extension to the penetration depth achievable in Raman spectroscopy of turbid media was recently accomplished by utilising the diffuse component of light in analogy to NIR absorption tomography[2] or fluorescence spectroscopy[3] where corresponding concepts are widely used. This article reviews recent developments in this area and gives examples of practical applications.

Propagation of light in diffusely scattering media

The principal barrier preventing conventional optical analytical methods from interrogating deep layers of tissue in disease diagnosis is the highly scattering nature of tissue. This prevents the formation of optical images required by conventional approaches such as confocal Raman microscopy to facilitate their depth discriminating capability. The same applies to the probing of powders. Photon propagation in such media, in the absence of strong absorption, as is typically the case of NIR Raman spectroscopy, is governed principally by diffuse scattering,[2] an analogous process to, for example, the diffusion of molecules in solutions. Fig. 3 depicts the three main components of light that can be defined in the propagation of light through diffusely scattering media: ballistic, snake and diffuse light, as introduced by Alfano *et al.*[2] The ballistic light is the part of light that is not scattered by the medium. The ballistic light intensity decreases exponentially with depth. Upon propagation through a turbid medium, this component gradually converts to the snake light, which in turn converts to the diffuse component. The snake component is only weakly deviated from its original direction by the scattering events, due to the fact that it only undergoes a small number of scattering events that are, typically, strongly biased towards the forward direction. This component also undergoes an exponential decay with depth, although its penetration depth is higher than that of the ballistic component. Both components can be utilised to form sharp or fuzzy images of objects in these media. This is crucial in applications such as confocal microscopy where the passage of light through a confocal aperture serves as a means for depth discrimination of the measured Raman signal.[1] An object viewed in the ballistic or snake light would appear transparent or semi-transparent, respectively.

The component penetrating the deepest, and consequently of the highest importance to the spectroscopic investigations of

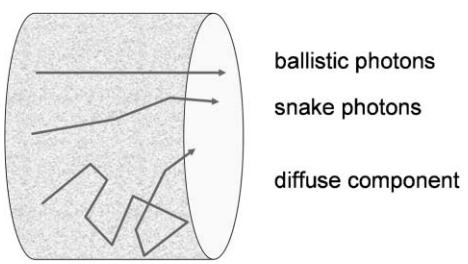

Fig. 3 Three main light components within turbid media.

deep layers of turbid media, is the diffuse component of light. In tissue, it penetrates to depths of up to several centimetres, in the NIR region of the spectrum, as opposed to the hundreds of micrometres or few millimetres of the ballistic and snake components. It is formed from the other components through a large number of scattering events, which completely randomise the photon direction. Such a photon, which 'forgets' its original direction, is of little use in conventional image-forming optical instruments for depth resolution. These photons often create large undesired backgrounds, and consequently noise, swamping the ballistic and snake components of light entirely. In the light of such a component, an object would appear translucent.

In terms of the theory of photon propagation, or migration in turbid media, the mean distance between individual scattering events is defined as the scattering mean free path (l_s) and the propagation distance over which the photon direction ultimately deviates significantly from its original direction of propagation is defined as the transport mean free path (l_t).[2] Due to the strong forward bias of the individual scattering events, the transport mean free path is typically an order of magnitude larger than the scattering mean free path; the relation is $l_s = (1 - g)l_t$, where g is defined as the anisotropy for the individual scattering event.

Recently, several effective methods based on Raman spectroscopy, capable of probing much deeper layers in diffusely scattering samples, have been developed. This progress stems from earlier photon migration investigations[2,4] and from the realisation that the Raman component decays substantially more slowly than its elastically scattered counterpart (*i.e.* the laser light), an effect which offsets the inherent weakness of the Raman technique.[5,6] This is due to the fact that Raman photons (unlike the elastic component of light) are not present in the medium from the beginning of the migration process, but instead are generated from the elastic component with a probability linearly dependent on the time the photons spend in the medium, *i.e.* the overall photon beam path. Therefore the Raman component undergoes not only decay due to diffuse scattering (and absorption if present), as does the elastic component, but in addition also undergoes regeneration from the elastic counterpart upon the propagation through the medium. This partial rejuvenation leads to a slower decay of the Raman signal with propagation distance in comparison with the elastic component, which is present from the very onset at its maximum strength and then decays monotonically away.[5] Of course, it must be realised that the strength of the elastic component is massively higher than that of the Raman signal, with Raman light being often present at extremely low levels necessitating very sensitive detection at near-single photon counting levels using, for example, cooled CCD (charge coupled device) detectors.[1] The application of the photon migration concept to Raman spectroscopy has led to the development of two principal non-invasive concepts, temporal and spatial.

2. Temporal approach

The discrimination of layers within a stratified turbid sample using the temporal approach is based on impulsive Raman excitation and fast temporal gating of the Raman signal (see Fig. 4). The experiments are typically performed in backscattering geometry, where the laser deposition and Raman collection points overlap on the sample surface. This concept relies on the simple fact that photons emerging from deeper layers of the probed turbid medium have to traverse larger distances *via* diffuse migration than the photons generated at shallower depths. Signals emerging from depths of several millimetres within turbid media can typically be spread over tens or even hundreds of picoseconds, in the absence of absorption, due to the random nature of diffuse scattering. Individual photons deposited at the near-surface layer are scattered randomly in all directions, undergoing a relatively slow forward 'random walk' in the medium. The process of Raman migration consists of two distinct phases; firstly, laser probe photons have to migrate to a given sample depth and, secondly, Raman photons created at this depth have to undergo a reverse diffusion process to reach the sample surface, if the backscattering collection geometry is used.

The ability to image an object in a turbid medium using temporally resolved Raman light was first demonstrated by Wu *et al.*[4] who measured the earliest arriving Raman photons in the light of a Raman component of β-carotene. The experiments were performed using photon counting detection with a time resolution of 80 ps. The time-resolved Raman signal of the β-carotene sample cell was detected at depths of several centimetres in a semi-turbid medium with a 7 mm scattering mean free path.

The full recovery of the Raman spectrum of a deeply buried layer in a turbid sample was first demonstrated by Matousek *et al.*[7] on a two-layer powder sample, building upon preceding work on Raman Kerr gated spectroscopy by Matousek *et al.*[8] and ground-breaking Raman photon migration investigations by Everall *et al.*[5] and Morris *et al.*[9] The sample consisted of a 1 mm optical path cuvette filled with PMMA (poly(methyl methacrylate)) spheres of $\sim$20 μm diameter, followed by a *trans*-stilbene tablet. The probe wavelength was 400 nm. The repetition rate of the laser system was 1 kHz and the Raman Kerr gate width was around 4 ps. The experimental scheme is shown in Fig. 5 and the results depicted in Fig. 6. The top spectrum is that obtained without the Kerr gate and contains contributions from both layers. Without prior knowledge of the individual components, a conventional Raman spectrometer would not provide sufficient information to permit the separation of the pure layer signals from each other. The gated

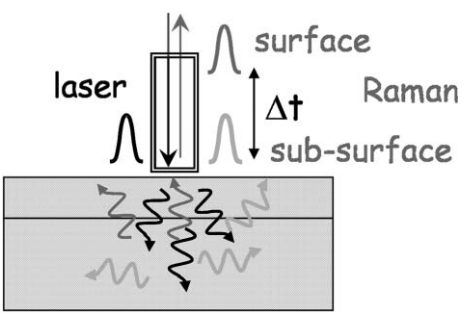

Fig. 4 Principal of the temporal concept for the discrimination of subsurface Raman signals.

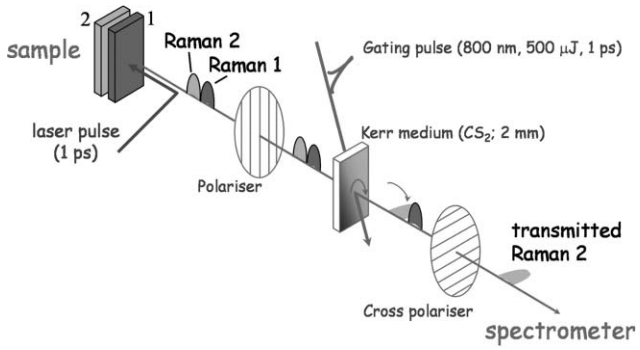

Fig. 5 Schematic diagram of the 4 ps Raman Kerr gated setup for the discrimination of subsurface layers. (Reprinted with permission from ref. 7. Copyright (2005) The Society for Applied Spectroscopy.)

Raman spectra are shown below. The early time delay spectra are dominated by the Raman spectrum of the top, PMMA layer. Only at 50 ps does one begin to discern a contribution from the stilbene sub-layer with its characteristic doublet at around 1600 cm^{-1}. The stilbene signal then continues to grow, peaking at around 200–300 ps before gradually decaying away. The PMMA signal on the other hand, drops off monotonically from 20 ps onwards and is absent above 100 ps.

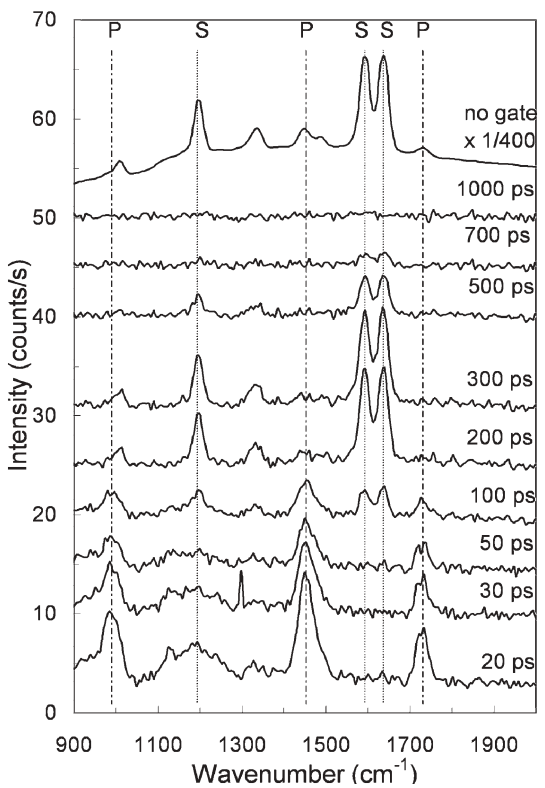

Fig. 6 The Kerr gated Raman spectra of a two-layer system consisting of a 1 mm-thick, PMMA layer made of 20 μm diameter spheres (P), followed by *trans*-stilbene powder (S). The spectra are plotted as a function of Kerr gate time delay. The top spectrum is obtained with no Kerr gating. The spectra are offset for clarity. The acquisition time was 200 s for each spectrum. The laser pulse energy was 5 μJ (*i.e.* average power 5 mW, 1 kHz repetition rate). (Reprinted with permission from ref. 7. Copyright (2005) The Society for Applied Spectroscopy.)

3. Spatial approach

3.1 SORS

Although proving to be an effective concept, the Raman Kerr gated approach has several inherent weaknesses precluding its wider deployment. Namely, it suffers from high instrumental complexity and cost, as well as from the requirement for the use of relatively high intensity laser pulses raising potential safety problems for *in vivo* biomedical applications. Recently, through collaborative efforts, an alternative, much simpler approach, spatially offset Raman spectroscopy (SORS),[10,11] was proposed and developed, relying solely on the spatial properties of the emerging Raman photons at the surface of the sample in analogy with tomographic concepts used widely in NIR absorption[2] and fluorescence spectroscopies.[3] The compatibility of this concept with lower-power continuous wave laser beams makes it instrumentally much simpler, as well as alleviates the above mentioned safety issues associated with the use of ultrashort laser pulses.

The proposed methodology is based on the collection of Raman spectra from regions of the sample surface that are spatially offset from the point of laser incidence (see Fig. 7). A set of Raman spectra obtained at different distances away from the laser deposition point contains different relative Raman contributions from layers located at different depths within the sample. This is due to the emerging Raman photons originating from different depths having different spatial distributions on the sample surface. The deeper layer Raman signal is spread over a wider area than that originating from shallower layers. This is a direct consequence of the fact that the deeper born photons have to traverse larger distances and on their way they diffuse sideways to a greater extent than the Raman photons originating from shallower layers. The same also applies to the laser photons that have to reach the target layer in the first instance.

The feasibility of this concept was first demonstrated by Matousek *et al.*[10] (see Fig. 8) on the same two-layer sample as that used in the aforementioned Kerr gated work[7] (see Fig. 5), *i.e.* a 1 mm-thick PMMA powder layer in front of a *trans*-stilbene powder layer, enabling a direct comparison between the two techniques. The results of these measurements with a 514 nm probe are shown in Fig. 9. For comparison, the Raman spectra of the pure layers measured in separate experiments are also displayed. The spectrum measured with the zero offset represents a conventional Raman measurement. A gradual

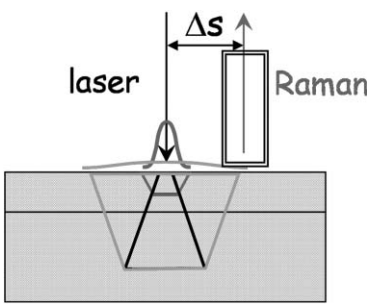

Fig. 7 Principal of the spatial, SORS, concept for the discrimination of subsurface signals.

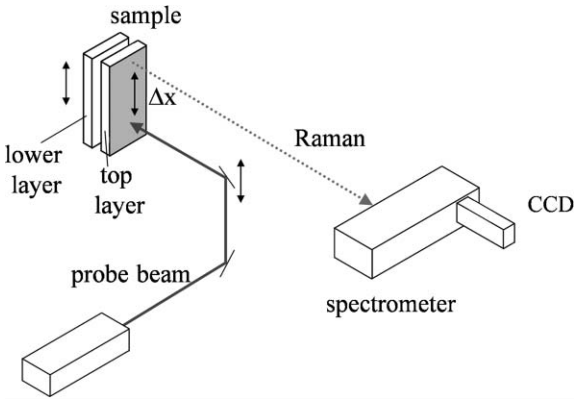

Fig. 8 Schematic diagram of a basic SORS experimental setup. (Reprinted with permission from ref. 10. Copyright (2005) The Society for Applied Spectroscopy.)

separation of the PMMA and *trans*-stilbene signals is accomplished using the SORS approach, by increasing the spatial offset. The surface Raman signal, PMMA, decays more rapidly than that of the lower layer, *trans*-stilbene. At distances of >2 mm, an order of magnitude improvement in the intensity ratio is achieved; the same work also reports that at a 3.5 mm spatial offset the relative ratio between the Raman signals of the two layers was improved by a factor of 19 whilst still obtaining good subsurface signals.

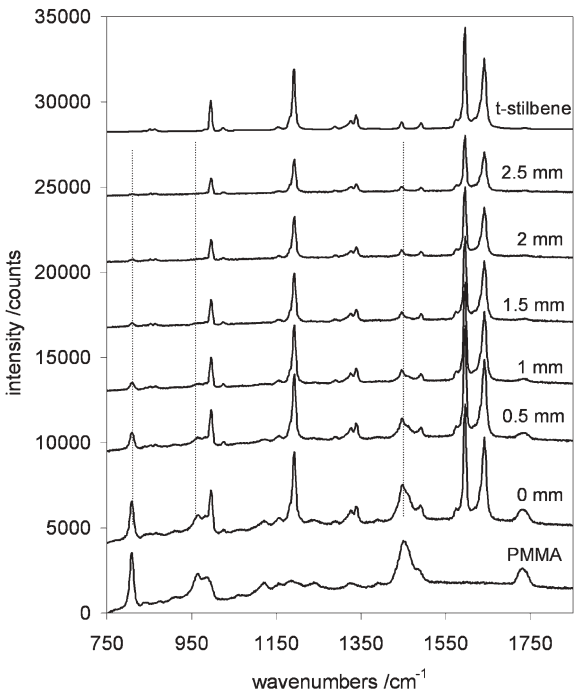

Fig. 9 A set of SORS spectra collected from a two-layer system consisting of a 1 mm-thick layer of PMMA made of 20 μm diameter spheres, followed by a 2 mm-thick layer of *trans*-stilbene powder, measured using 514 nm as the probe wavelength. The spectra are shown for different spatial offsets. The top and bottom spectra are those of the individual layers obtained in separate measurements. The spectra are offset for clarity. The acquisition time was 100 s for each spectrum and the average laser power 12 mW. (Reprinted with permission from ref. 10. Copyright (2005) The Society for Applied Spectroscopy.)

In comparison with the Kerr gated work, the signal quality attained in the SORS measurement was, despite its instrumental simplicity, substantially higher. This is due to the fact that the spatial gating technique integrates all the Raman signals across the entire time domain, unlike the temporal approach, where the ultrafast gating (4 ps) results in a severe reduction in the detected signal due to the narrow temporal slicing of relatively long Raman signals.

For a two-layer system the detected Raman spectra can be further separated from each other to produce pure Raman spectra of individual layers using a simple scaled subtraction of two spectra obtained at different spatial offsets. If a stratified sample with more than two layers is present, as is often the case with biological samples, then multivariate data analysis of a more extensive data set is required. This can be accomplished, for example, using principal component analysis (PCA) followed by band target entropy minimisation (BTEM)[12] factor analysis. For the effective resolution, as a rule of thumb, one typically needs to collect 10*n* Raman spectra where *n* is the number of distinct layers. Crucially, the BTEM method can be accomplished with no *a priori* knowledge of the system composition, which is a common feature of self-modelling curve resolution procedures to which this method belongs to.

The coupling of the SORS concept with fibre optic technology developed earlier by Ma and Ben-Amotz,[13] yields dramatic enhancements to its sensitivity. This was experimentally demonstrated with SORS by Schulmerich *et al.*,[14] who utilised a commercial fibre probe with so-called global illumination configuration,[15] and subsequently by Matousek *et al.*,[16] who used fibres arranged on annuli of different radii (see Fig. 10), with each different radius being presented to a different horizontal section of a two-dimensional CCD detector. This enables the sensitive probing of deep layers of tissue, even at low illumination powers such as those required for the safe illumination of skin. The work of Schulmerich *et al.*[15] also demonstrated for the first time the feasibility of SORS based tomography, thus opening potential new imaging techniques for probing subsurface structures using Raman light.

It is also noteworthy that the SORS approach is capable of effectively suppressing not only Raman signals from the

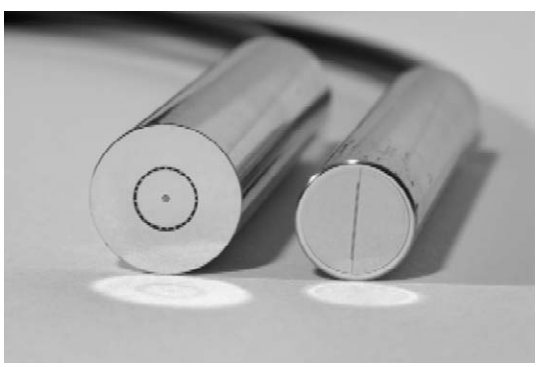

Fig. 10 A photograph of the SORS ring fibre probe (left: input side; right: output side). (Reprinted with permission from ref. 16. Copyright (2006) The Society for Applied Spectroscopy.)

surface layer but also the interfering fluorescence originating from surface layers as fluorescence signals have the same spatial, but not temporal, dependence as the Raman signal originating from the same layer. This feature is beneficial in a number of applications, including *in vivo* spectroscopy where melanin components located at the skin surface often induce large amounts of fluorescence backgrounds, preventing sensitive interrogation of subsurface structures with conventional Raman spectroscopy. Another area to benefit is the probing of pharmaceutical tablets and capsules, which often possess fluorescing surface layers.

3.2 Inverse SORS

Although the SORS ring fibre probe proved to be a very effective analytical tool for subsurface Raman spectroscopy, it possesses some inherent limitations preventing exploitation of the full potential offered by the SORS concept. One of the main problems stems from the way the Raman spectra of different spatial offsets are registered on the detector. With the ring fibre probes, multiple Raman spectra are typically collected on different CCD detection tracks. Such spectra exhibit small distortions due to spectrograph imaging imperfections. Although some numerical compensation is possible, their complete elimination is practically impossible. These become particularly apparent if the spectra from different tracks are scaled and subtracted from each other, a procedure involved in the post-processing of SORS spectra to recover pure Raman spectra of individual layers, resulting in artefacts resembling difference-like spectra. This feature limits the sensitivity of the technique and consequently its capacity to recover weak Raman signals from deep layers of sample.

This drawback can be eliminated by adopting a reverse delivery–collection geometry, inverse SORS, proposed and demonstrated independently by Matousek[17] and Schulmerich *et al.*[18,19] In this concept, Raman light is collected through a group of fibres tightly packed at the centre of the probe. These can be randomly organised and binned on the CCD into a single spectrum.[17] The laser probe beam is brought on to the sample in the form of a ring of a given radius centred at the collection zone (see Fig. 11). The artefact issue is eliminated as all the Raman spectra are subject to the same imaging distortions and collected through the same set of CCD pixels.

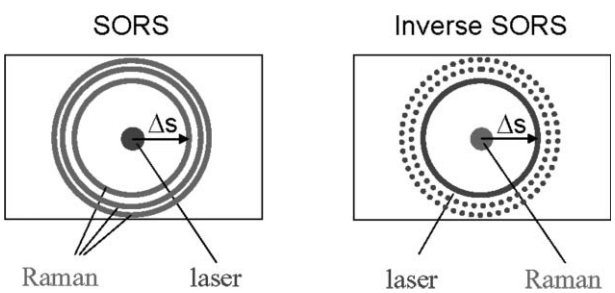

Fig. 11 Schematic diagram of conventional SORS and inverse SORS concepts showing Raman collection and laser beam delivery geometries. (Reprinted with permission from ref. 17. Copyright (2006) The Society for Applied Spectroscopy.)

The ring beam can be generated using an axicon (conical lens) and the SORS spatial offsets attained by varying the radius of the ring illumination zone by changing the axicon-to-target distance[17] or by varying the magnification of a telescope incorporated in between the sample and axicon.[18]

The experimental demonstration of the higher sensitivity available with this concept, by probing a 2 mm-thick PVC pipe with a paracetamol tablet placed behind the pipe wall, is shown in Fig. 12.[17] The experiment was performed both in the inverse SORS and normal SORS fibre ring collection geometries for comparison. The inverse SORS spectrum is clearly of superior quality, exhibiting no artefacts after the scaled subtraction and revealing the clear Raman spectrum of paracetamol in contrast to that of normal SORS which is littered with subtraction artefacts.

An additional, crucially important benefit of inverse SORS is that it has an enhanced available illumination area through which the laser beam can be delivered into the sample. Consequently, higher laser powers can be employed. This is vital for *in vivo* spectroscopy where safe illumination intensity limits must be adhered to.

A final advantage of this concept is the ability to set an arbitrary value of the spatial offset, enabling optimisation of the experimental parameters for different sample types. This is not possible with the SORS ring fibre probes, where spatial offsets are fixed as the tracks are built into the probe.

3.3 Transmission Raman

For some analytical applications involving diffusely scattering media, the primary target of analysis can be the overall bulk content of the sample rather than the composition of individual layers or sample microstructure. An example is the chemically specific analysis of pharmaceutical tablets to identify the overall tablet bulk content. Matousek and Parker[20] recently demonstrated that a transmission Raman geometry is particularly well suited for such analysis. In this approach, the laser beam is brought onto the sample from one side and the Raman signal collected from the opposite side. This concept can be considered to be a special case of SORS, in which the laser beam and Raman collection points are displaced to the extreme by being on opposite sides of the sample.

This work demonstrates the gross insensitivity of the transmission geometry to the depth of the probed layers, in comparison with the conventional backscattering Raman mode. This feature was confirmed using Monte Carlo simulations. The results show that the collection of Raman signals in conventional backscattering geometry leads to an extremely strong bias towards the surface layers of the sample (see Fig. 13). The plot indicates that at a depth of 3 mm the Raman signal originating from an inter-layer, *e.g.* impurity, drops by 4 orders of magnitude from its original level at the zero depth. In contrast, the transmission geometry is largely insensitive to the depth of the impurity layer. Consequently, the transmission geometry provides a substantially more uniform way of probing the overall sample content.

The transmission Raman concept is applicable to the bulk probing of pharmaceutical tablets in quality control

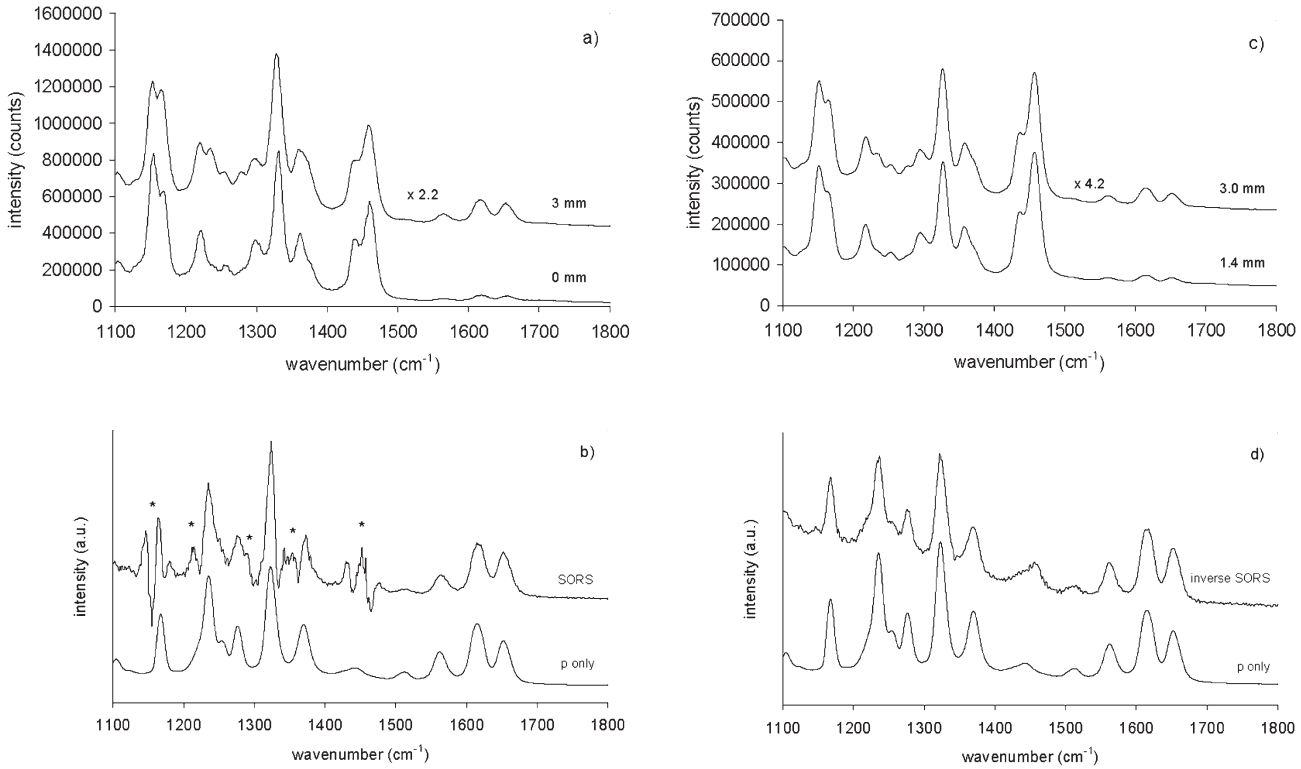

Fig. 12 Comparison of the performance of (a, b) conventional SORS and (c, d) inverse SORS in the recovery of a subsurface Raman spectrum. The experiments were carried out using a standard paracetamol tablet placed behind a 2 mm-thick white PVC wall. Raw Raman spectra obtained with two different spatial offsets are shown in the top frames. The recovered subsurface Raman spectra, along with the pure Raman spectra of paracetamol ('p only') obtained separately, are shown in the bottom frames. The acquisition times were 20 s for the conventional SORS and 10 s for the inverse SORS measurements. The laser power was 50 mW. The spectra are offset for clarity. Subtraction artefacts are marked with asterisks. (Reprinted with permission from ref. 17. Copyright (2006) The Society for Applied Spectroscopy.)

applications, the probing of colloidal liquids in the pharmaceutical or chemical industries and to the deep probing of human tissue. In many of these applications, it is also beneficial that the concept very effectively suppresses Raman and fluorescence signals originating from thin surface layers of the probed sample, in contrast with conventional backscattering Raman geometry.[21]

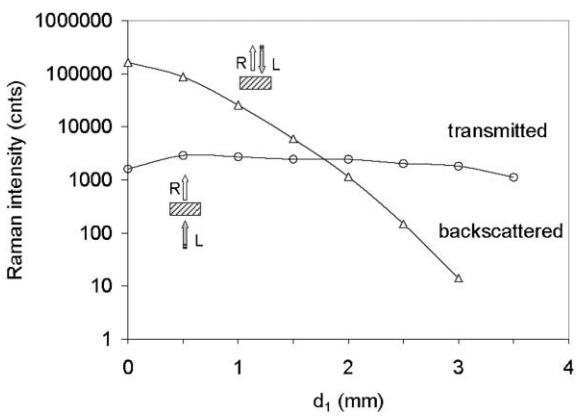

Fig. 13 Plot of Raman intensities for the backscattering and transmission geometries *versus* depth of the inter-layer (impurity) within a pharmaceutical tablet-like medium. The dependencies are the results of Monte Carlo simulations. (Reprinted with permission from ref. 20. Copyright (2006) The Society for Applied Spectroscopy.)

4. Examples of application areas

4.1 Biomedical applications

4.1.1 Probing of bones through skin for disease diagnosis. A major clinical demand for bone quality assessment arises from the diagnosis of osteoporosis.[9,22,23] Currently, dual-energy X-ray absorptiometry (DEXA) represents the gold standard screening for this disease. Although widely used, its accuracy in assessing bone strength is only 60 to 70%. This is believed to be due to the fact that the technique can only probe the density of the mineral component, constituting around two thirds of bone mass. However, the remaining component (mainly collagen) also contributes to bone strength but remains invisible to DEXA. Both infrared and Raman spectroscopies have been shown to be capable of providing useful information on both the components *in vitro*. Recently, both the temporal and spatial approaches have been applied successfully to the non-invasive interrogation of bones, building on the pioneering work of Morris *et al.*[9]

Temporal approach. The collaborative team of Draper[22] reported the use of the temporal approach in the non-invasive assessment of bones using mouse samples. In these experiments, 1 ps laser pulses at 800 nm (1 kHz) were used as a probe, with a 4 ps Raman Kerr gate in the detection system. As the signs of osteoporosis in Raman spectra were expected to be

subtle,[23] in this initial study, animals with *osteogenesis imperfecta* were used instead, as this disease exhibits greater changes to the bone matrix. Mouse forelimbs were used and comparative measurements were performed on matched wild type, *i.e.* healthy mouse samples. The depth of the bone from the skin surface was around 1 mm. The non-invasive measurements were repeated on the corresponding excised samples.

Typical Raman spectra from bone are well established. Specific regions are associated with the mineral and organic phases, respectively. For details, the reader is referred to the work of Carden and Morris.[24] Non-invasive Raman spectra (see Fig. 14) revealed a considerable difference between the two genotypes, in particular, in the ratio of the phosphate (at 958 cm^{-1}) to collagen ($\sim$1450 cm^{-1}) band intensities. These differences were satisfactorily reproduced by measurements on excised bones.

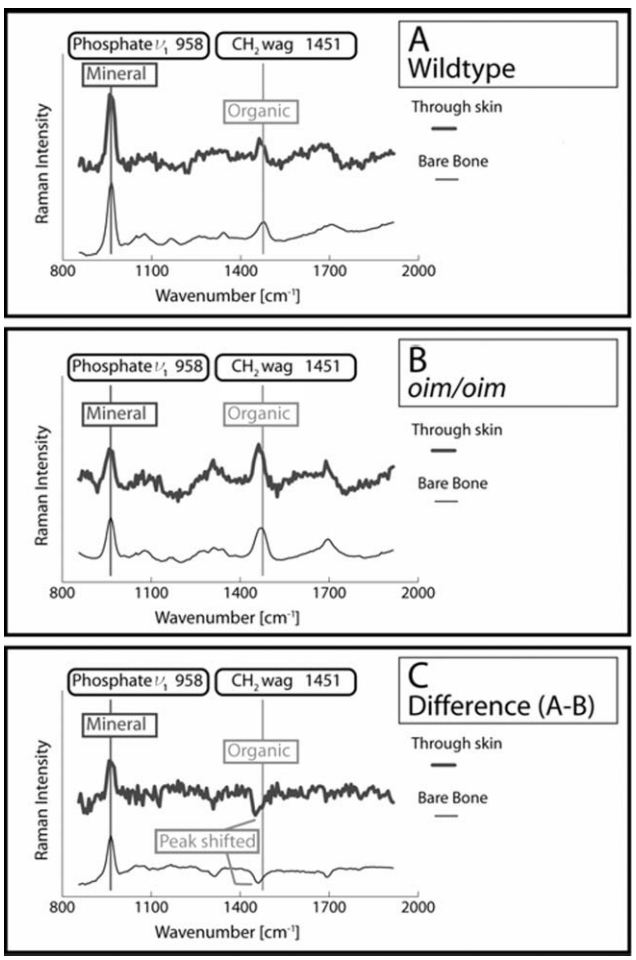

Fig. 14 Raman spectra of bone measured from two genotypes; wild type mice and *osteogenesis imperfecta* (*oim*/*oim*) mice. The spectra were recorded both through the overlying skin and directly on bare bone using the ultrafast Raman Kerr gating method. (A) Raman spectra of wild type mice; (B) Raman spectra of *oim*/*oim* mice; (C) the difference Raman spectra obtained by subtracting the spectra from the two genotypes. The acquisition times were between 7 and 15 min for each spectrum and the laser pulse energy was 340 μJ (average power 340 mW, 1 kHz repetition rate). (Reproduced from ref. 22 with permission of the American Society for Bone and Mineral Research.)

The study demonstrated that the major components of the Raman spectrum of bone can be detected through overlying tissue. Although all the key Raman features of bone are clearly visible, there is appreciable noise present in the non-invasive spectra, precluding more detailed examination for weaker spectral features such as those, for example, expected to be due to osteoporosis as demonstrated by McCreadie *et al.*[23] The work represents a milestone in the non-invasive Raman spectroscopy of bone, demonstrating for the first time the feasibility of such an approach and paving the way for further studies and developments in this area.

Despite the progress made, large issues still remained to be resolved following this study before the technique could be applied to probing human tissue *in vivo*. The main issue is the fact that to reach the required signal-to-noise (S/N) within the spectra required the use of peak laser intensities two to three orders of magnitude higher than those permissible for safe illumination of human skin as defined by the laser safety standard.[16] On a less severe point, the complexity and cost of the associated laser instrumentation also prevents its wider applicability. Both these limitations were subsequently lifted by the development of the SORS concept, which requires the use of continuous wave laser beams only, thus reducing issues with maximum permissible exposures and drastically reducing the complexity of the associated instrumentation.

Spatial approach. The advent of the SORS concept opened new prospects for the development of more simple and skin-safe instruments capable of interrogating bones under the skin at clinically relevant depths. The first demonstration of the SORS concept in the area of non-invasive Raman spectroscopy of bones was performed by Schulmerich *et al.*[14] In this work, the team recovered the Raman spectra of bones non-invasively from depths of several millimetres in animal and human cadaver samples. In their subsequent research, with much improved instrumentation based around the ring illumination geometry (equivalent to inverse SORS), Schulmerich *et al.*[18] reached another major milestone by demonstrating the ability to recover spectra with better than 8% accuracy in terms of the relative Raman band intensities between the phosphate (958 cm^{-1}) and carbonate (1070 cm^{-1}) bands, from a depth of 4 mm from chicken tibia. This achievement is highly significant as the successful detection of osteoporosis is likely to require this level of accuracy, as indicated earlier by McCreadie *et al.* on excised bones.[23] The success is due to both the improvement in detection methodology, permitting higher energy to be deposited to the sample, without damage, using the ring-illumination approach, and to the use of the robust factor analysis routine, BTEM, which is well suited to the problem of separating multilayer signals in SORS measurements.[18] The results of these experiments are shown in Fig. 15. The measurements were performed using 785 nm as the probe wavelength. The spectra were collected using a fibre probe and the laser beam was deposited using an axicon with a cone angle of 179.5°.

In subsequent research using SORS, Matousek *et al.*[16] demonstrated the potential of recovering the Raman spectra of bones from humans *in vivo*. Although the obtained spectra were of limited quality given the low power used, the

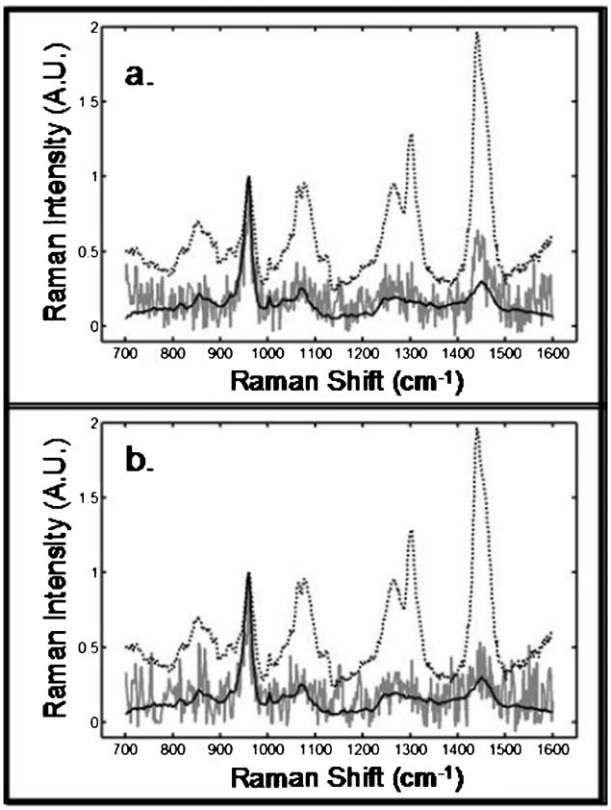

Fig. 15 Measurements made through 4 mm of overlying tissue on a chicken tibia at the mid-diaphysis using the SORS approach. Transcutaneous (···); recovered bone factor (gray); and exposed bone (black). (a) Recovered bone factor using data from all 50 collection fibres; and (b) recovered bone factor using data from the 32 innermost collection fibres. The laser power was 110 mW and the acquisition time 120 s. (Reprinted with permission from ref. 18. Copyright (2006) The Society of Photo-Optical Instrumentation Engineers.)

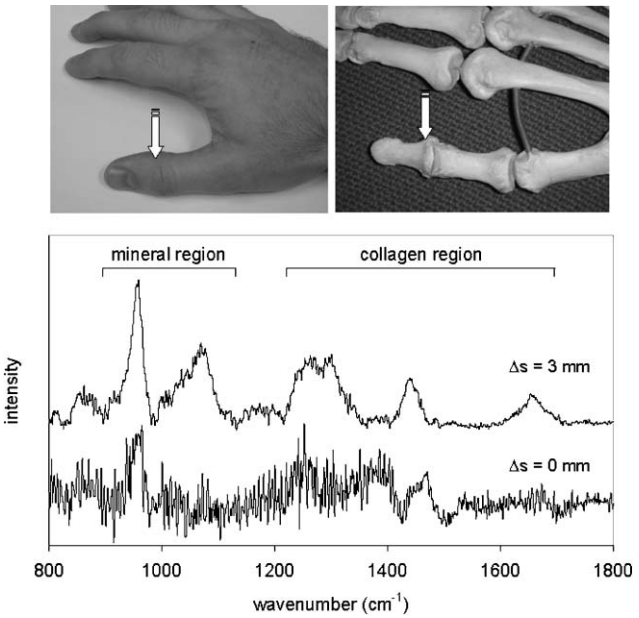

Fig. 16 The raw SORS spectra for the zero and 3 mm spatial offsets from the non-invasive transcutaneous measurement of human bone *in vivo* at the distal phalanx of the thumb. The spectra were obtained using a continuous wave laser operating at 827 nm with skin-safe laser power (2 mW). The spectra are offset for clarity. The acquisition time was 200 s. (Reprinted with permission from ref. 16. Copyright (2006) The Society for Applied Spectroscopy.)

experiments demonstrated that the key bone features can be obtained with SORS *in vivo* under safe illumination conditions. The measurements were performed using the ring fibre probe shown in Fig. 10. The collected raw spectrum (before the removal of the remaining soft tissue signal), with 3 mm spatial offset, with fluorescence background subtracted, is shown in Fig. 16, along with a corresponding conventional Raman spectrum obtained at zero spatial offset. The spectra were collected from the thumb distal phalanx bone of a volunteer through around 2 mm of overlying soft tissue. The overall acquisition time was 200 s and the probe wavelength was 830 nm. The laser beam area on the sample was 1.1 mm^2 and the laser power was attenuated to 2 mW, *i.e.* to well within the maximum permissible exposure limit. The comparative conventional Raman spectrum suffers from excessive noise, stemming from high fluorescence background mainly originating from melanin components in skin. This interference was effectively suppressed with the SORS method. Although the SORS spectra are still likely to contain an appreciable amount of overlying tissue signals, the key bone spectral features are visible. Further decomposition into pure spectra of individual layers was performed by scaled subtraction of Raman spectra obtained at different spatial offsets, although the accuracy achieved in this work did not reach the level required for the diagnosis of conditions such as osteoporosis.[23] Nevertheless, the aforementioned experiments provided another important stepping stone for further work and stimulated further development of the SORS concept capable of yielding much more cleanly decomposed spectra.[17,18]

4.1.2 Chemical identification of calcifications in breast cancer lesions. Work by Baker *et al.*[25,26] and Matousek and Stone[27] demonstrates the potential of the use of Kerr gated, SORS and transmission Raman concepts in the probing of deeply buried calcifications within breast tissue, achieving penetration depths of 0.9, 8.7 and 16 mm in chicken breast tissue phantoms, respectively. Calcifications identified by mammography can indicate the presence of a malignant breast lesion, although the mammographic technique cannot detect their chemical constituency which is indicative of the disease state. For this, a biopsy is often required, bringing about an associated high medical cost stemming, in part, from the fact that 70–90% of mammographically detected lesions are found to be benign upon needle biopsy.

As described earlier in a pioneering work by Haka *et al.*,[28] microcalcifications can be divided into two types; type I, consisting of calcium oxalate dihydrate (cod), and type II deposits, containing mainly calcium hydroxyapatite (hap). Calcium oxalate crystals are mainly found in benign ductal cysts and rarely in carcinoma, and calcium hydroxyapatite crystals are found both in carcinoma and in benign breast tissue. In addition, it has been found that type II calcifications present in benign cysts are spectroscopically distinct from type II calcifications found in malignant lesions.

Since different types of calcifications exhibit chemical differences, significant insight may be gained by using non-invasive Raman spectroscopy as a diagnostic tool. Raman spectroscopy holds particular promise for addressing this problem as the Raman scattering cross-section of calcifications is substantially higher than that of the soft surrounding tissue. In addition, it has recently been shown that Raman spectroscopy is capable of distinguishing between the two types of calcification in excised breast tissue.[28] However, until the advent of SORS, Raman spectroscopy could be applied to probing tissue in depths of up to only several hundred micrometres.

In contrast, the new non-invasive Raman methods open the potential for deep non-invasive monitoring of calcifications at depths of up to a centimetre or so. To date, the concept that showed the greatest potential is the transmission Raman geometry, yielding the greatest penetration depth for the monitoring of calcifications in breast tissue.[27] This technique, as well as exhibiting gross insensitivity to the depth of the probed calcifications, also suppresses signals originating from the surface layers of tissue, such as melanin fluorescence. In contrast, conventional backscattering Raman spectroscopy accentuates such surface signals. The transmission Raman geometry is also compatible with breast mounts used in conventional mammography.

The transmission Raman experiments reported by Matousek *et al.*[27] were performed using 830 nm as the probe wavelength, with a laser beam diameter at the sample of around 4 mm. The Raman light was collected using a fibre bundle consisting of 33 fibres. The study was performed on a phantom constructed using a 16 mm slab of chicken tissue with a thin layer (100–300 μm) of calcified material smeared in the middle of the tissue. The results are summarised in Fig. 17. Despite the presence of substantial noise, identifiable Raman spectra of individual calcified compounds were clearly recovered. Although the amount of calcification material used

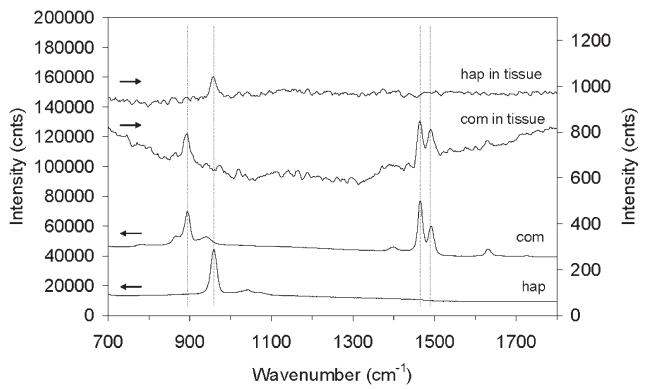

Fig. 17 Raman spectra of two types of calcified materials (a 100–300 μm thick layer) recovered from a 16 mm-thick slab of chicken tissue ('hap in tissue', 'com in tissue'). The spectra were obtained by subtracting raw transmission Raman spectra of tissue only from those of tissue containing calcified material. The pure Raman spectra of individual calcified materials are also shown. The acquisition time was 100 s, with a laser power of 60 mW. The spectra are offset for clarity. (Reprinted with permission from ref. 27. Copyright (2007) The Society of Photo-Optical Instrumentation Engineers.)

is estimated to be two orders of magnitude above clinically relevant levels, further improvements of the technique (bringing its sensitivity to clinically relevant levels) are believed to be feasible. If this goal could be achieved, the technique would likely play an important role in breast cancer diagnosis, potentially being used in conjunction with mammography or ultrasound techniques to enhance their diagnostic potential.

4.2 Probing of pharmaceutical products

4.2.1 Probing of pharmaceutical tablets in quality control. Some pharmaceutical quality control applications require probing of the bulk content of a sample rather than its micro- or layered structure. The need for such information stems from the fact that it is the overall content of the tablet delivered during medical treatment that must be accurately known as any improper heterogeneous components concealed within the tablet may have harmful effects. Ideally, the content information should be obtained in a non-destructive manner and on short time scales, as is required in environments such as production lines.

Raman spectroscopy is a proven valuable tool for compositional analysis of pharmaceutical tablets,[1] although in its backscattering mode it is excessively biased to the surface layers of the probed medium. Work by Matousek and Parker[20] overcomes this bias by using the transmission Raman approach to provide detailed spectroscopic information about the sample throughout its entire depth. The feasibility of this concept was demonstrated both numerically and experimentally. The experimental demonstration was performed both in the conventional backscattering geometry and in transmission mode on a standard paracetamol tablet with a simulated impurity layer placed at the extreme locations of the tablet, *i.e.* at the front and back. The tablet used had a thickness of 3.9 mm. The impurity layer consisted of a 2 mm fused silica cuvette filled with *trans*-stilbene powder. The experiments were performed using an 830 nm probe, with a laser beam diameter of 4 mm. Raman light was collected using a fibre probe consisting of 7 fibres.

The results of this measurement are shown in Fig. 18 and demonstrate the surface layer bias of the conventional backscattering geometry as only the Raman spectrum of the illuminated side of the probed object can be detected with no trace of the layer placed at the opposite side. In contrast, in the transmission geometry gross insensitivity is seen to the location of the impurity layer. Irrespective of the orientation of the sample, *i.e.* whether the impurity layer is at the front or back of the sample, its Raman signature is clearly detectable with a similar level of sensitivity.

For the tablet alone, the overall Raman signal intensity when going from the conventional backscattering to transmission geometry was reduced by only a factor of 12. In addition, a good Raman signal could also be observed through 2 tablets placed back-to-back.

The large illumination areas feasible in transmission geometry also make it possible to use substantially higher laser powers and further reduce exposure times, potentially down to a fraction of a second. These properties, in combination with the technique's high chemical specificity

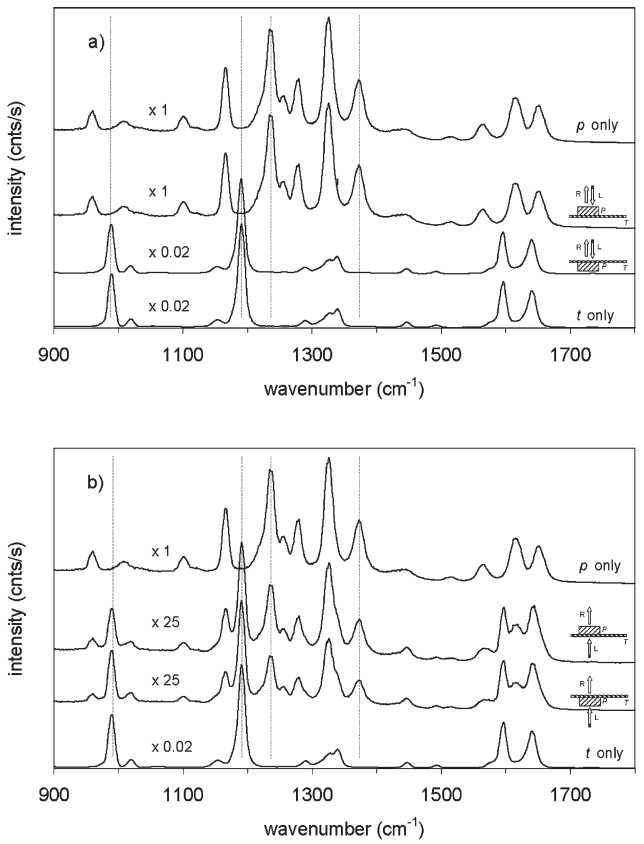

Fig. 18 The Raman spectra obtained from a two-layer sample (3.9 mm-thick paracetamol tablet and 2 mm-thick *trans*-stilbene powder 'impurity' layer) using (a) conventional backscattering geometry; and (b) transmission geometry. The measurements are performed at two sample orientations, with paracetamol at the top and bottom of the *trans*-stilbene cell as indicated in the graphs. The top and bottom spectra are those of paracetamol and *trans*-stilbene, respectively, obtained in separate experiments. The acquisition times were between 0.2 and 10 s, with a laser power of 80 mW. The spectra are offset for clarity. Legend: p: paracetamol; t: *trans*-stilbene; R: Raman light; L: laser beam. (Reprinted with permission from ref. 20. Copyright (2006) The Society for Applied Spectroscopy.)

and simplicity, make the method particularly well suited for quality control applications.

4.2.2. Probing of pharmaceutical capsules in quality control. Some pharmaceutical applications require the non-invasive probing of capsules or coated tablets through their coating. Although the Raman technique has proven to be a valuable tool in this area too, when it comes to probing capsules of certain colours the Raman signal and fluorescence emanating from the capsule shell may interfere excessively with the Raman signal of the material held within the capsule, leading to a reduction of the technique's sensitivity.

Work by Matousek and Parker[21] demonstrates how the use of the transmission Raman geometry for weakly or non-absorbing diffusely scattering samples can dramatically reduce this surface layer interference, permitting detailed spectroscopic information on the interior composition of the capsule to be obtained. The experiments were performed with 830 nm as the probe wavelength and the laser spot diameter was ~4 mm in transmission geometry and ~0.5 mm in the comparative backscattering and SORS geometries. In the conventional Raman backscattering and the transmission Raman measurements, the Raman light was collected using a fibre bundle probe consisting of 7 fibres tightly packed at the centre of the probe. The SORS comparative measurements were carried out using 26 fibres distributed on a ring of 3 mm radius representing a 3 mm spatial offset.

Fig. 19 compares the performance of the three non-invasive Raman approaches, SORS, conventional backscattering Raman and transmission Raman geometries, on a highly fluorescent capsule. The spectra are shown in their raw form with no backgrounds removed. It is evident that both the SORS and the transmission geometry permit the observation of the Raman signals, even if these are completely obscured by fluorescence originating from the capsule shell in the conventional backscattering Raman measurement. Furthermore, it is clear that the transmission geometry improves on the SORS approach in terms of signal quality, although larger SORS spatial offsets should provide spectra of similar quality. Similar performance is expected to be obtained with coated tablets.

4.2.3 Drug authentication. Due to the increasing volume of counterfeit drugs entering the distribution chain there is a growing need for effective means of non-invasive verification of the authenticity of pharmaceutical products.[29] For example, the infiltration of the market by fake antimalarial drugs currently presents a major crisis in eastern Asia and poses a serious threat to life.

Although NIR absorption spectroscopy is used in this application, its limited chemical specificity restricts its effectiveness. Raman spectroscopy used in the backscattering collection geometry is an alternative technique that is increasingly used in this area, mainly due to its high chemical specificity. However, in some instances, and in particular with darkly coloured coatings or capsules or thick packaging, this geometry can yield excessively intense Raman signals or fluorescence originating from the surface layers, reducing its sensitivity and, in extreme cases, completely swamping the Raman signal of pharmaceutical ingredients held within.

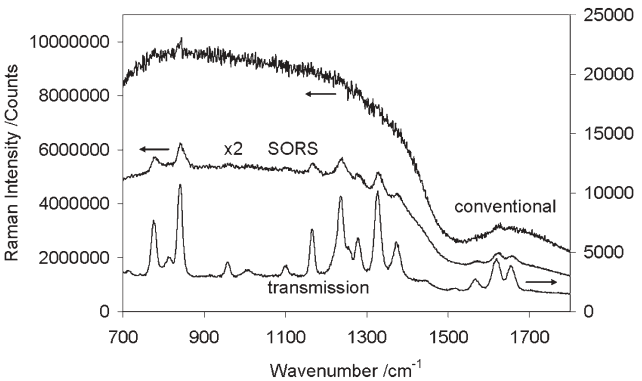

Fig. 19 The comparison of conventional backscattering, SORS and transmission Raman geometries in non-invasive probing of the green section of a Sudafed Dual Relief capsule of shell thickness 150 μm. The acquisition time was 10 s, with a laser power of 80 mW. (Reprinted with permission from ref. 21. Copyright (2007) John Wiley & Sons.)

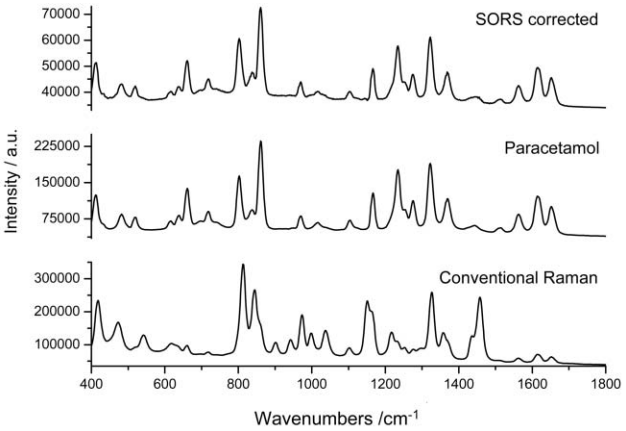

Fig. 20 Non-invasive Raman spectra of paracetamol tablets measured through a white, diffusely scattering 1.7 mm-thick plastic container in drug authentication. Conventional Raman and SORS raw data are shown, together with the tablets reference Raman spectrum. The acquisition time was 10 s and the laser beam power 50 mW. (Reprinted with permission from ref. 29. American Chemical Society.)

Work by Eliasson and Matousek[29] demonstrates the benefits of applying SORS in this area. The measurements were performed using the SORS point illumination and collection geometry on two types of widely used packaging, namely, blister packs and white plastic bottles. Comparative measurements were also performed in the conventional backscattering Raman geometry. In all the studied cases, SORS outperformed the conventional Raman technique through its substantially more effective suppression of the interfering Raman and fluorescence contributions originating from the packaging.

Fig. 20 shows the performance of SORS and conventional backscattering Raman geometry in the non-invasive probing of white plastic bottles containing pharmaceutical tablets. In this application, the conventional Raman approach was totally ineffective due to the overwhelming intensity of the Raman signal of the container. Even under these challenging conditions the SORS approach, after the scaled subtraction of two SORS spectra obtained at different spatial offsets (0 and 3 mm), yielded a very clean Raman spectrum of the pharmaceutical tablets. The experiments were performed at 830 nm probe wavelength and the laser spot diameter at the sample was $\sim$0.5–1 mm. A fibre bundle probe made of 22 fibres was used to collect Raman light.

The concept holds great promise for more accurate and sensitive identification of drugs in the supply chain. Its applicability, however, stretches well beyond this application area and is also well suited to the monitoring of substances held in diffusely scattering packaging in security screening applications.

4.3 Security applications

The recent heightened terrorist threat underlines the importance of the availability of robust security screening techniques with high chemical specificity. No single technique exists capable of addressing all the needs in this area, given the wide range of samples and containers encountered. Consequently, a multitude of techniques are used to address the problem effectively. In such applications, high throughput methods are often used as a first screening layer, with any problematic subjects being referred to the second, lower throughput, screening procedure. An example is the screening of envelopes at mail sorting centres.

4.3.1 Probing of envelopes. An article by Matousek[17] reports on the use of inverse SORS in the probing of powders held in envelopes and compares the results achieved with those attainable using conventional backscattering Raman spectroscopy. Similar results can also be achieved in the transmission Raman mode[30] as shown in Fig. 21. In these measurements, a standard brown envelope containing white sugar was used. Comparative conventional backscattering Raman measurements yielded only a massive fluorescence background, originating from the envelope material. In contrast, the transmission geometry shows clearly the Raman components of sugar held within the envelope. This example demonstrates the capability of the transmission Raman geometry to

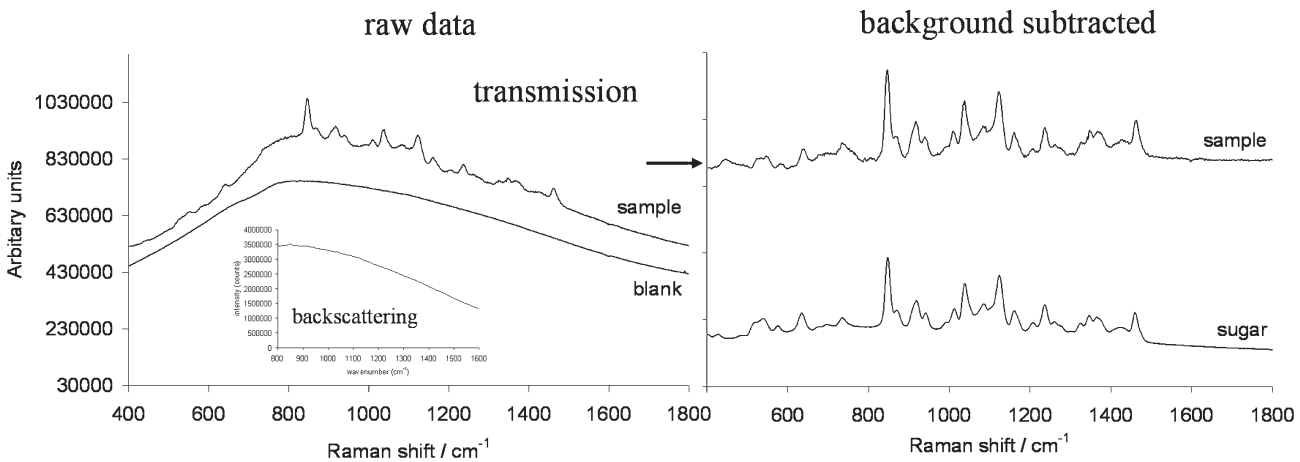

Fig. 21 Non-invasive measurement of powders in envelopes in security screening applications. The measurement was performed in transmission geometry with an envelope containing sugar representing a hidden illegal or harmful substance. The acquisition time was 10 s and the laser power 55 mW. The inset shows the result of a backscattering Raman measurement of the same sample.

substantially reduce not only contributions from the Raman spectra of surface layers but also fluorescence originating from the surface layers of the probed sample. The pure Raman spectrum of sugar contained within the envelope can be recovered by subtracting the fluorescence background, a task that can be, for example, performed by automated means.[31] The experiments were performed using 830 nm as the probe wavelength, with a probe beam diameter of 0.5 mm. The Raman signal was collected using a fibre probe consisting of 33 fibre elements.

5. Conclusions

The emergence of new non-invasive Raman spectroscopic techniques stimulates the birth of numerous new analytical methods for the non-invasive probing of diffusely scattering media at depths previously inaccessible. Although much work remains to be done, prospects for many new exciting applications are already looming on the horizon. These include the diagnosis of diseases such as osteoporosis, brittle bone disease and breast cancer, quality control and authentication of pharmaceutical products and security screening applications. These developments come at a time when Raman spectroscopy is completing its transformation from laboratory technique to practical analytical tool; a journey driven by recent advances in laser and detection technologies. Future developments of many of these new applications may exert a profound influence over our daily lives.

Acknowledgements

The author wishes to thank Professor Anthony Parker, Dr Darren Andrews, Dr Tim Bestwick, Dr Ian Clark, Dr Charlotte Eliasson, Dr Neil Macleod and Professor Mike Dunne of CCLRC for their support of this work. The author also wishes to thank to Professor Michael Morris (University of Michigan) and Dr Neil Everall (ICI PLC) for numerous fruitful discussions on the covered topics. The EPSRC is gratefully acknowledged for their support of this work (grant EP/D037662/1).

References

1 M. J. Pelletier, *Analytical Applications of Raman Spectroscopy*, Blackwell Science, Oxford, 1999.
2 B. B. Das, F. Liu and R. R. Alfano, *Rep. Prog. Phys.*, 1997, **60**, 227–292, and references therein.
3 T. J. Pfefer, K. T. Schomacker, M. N. Ediger and N. S. Nishioka, *Appl. Opt.*, 2002, **41**, 4712–4721, and references therein.
4 J. Wu, Y. Wang, L. Perelman, I. Itzkan, R. Dasari and M. S. Feld, *Appl. Opt.*, 1995, **34**, 3425–3430.
5 N. Everall, T. Hahn, P. Matousek, A. W. Parker and M. Towrie, *Appl. Spectrosc.*, 2001, **55**, 1701–1708.
6 N. Everall, T. Hahn, P. Matousek, A. W. Parker and M. Towrie, *Appl. Spectrosc.*, 2004, **58**, 591–597.
7 P. Matousek, N. Everall, M. Towrie and A. W. Parker, *Appl. Spectrosc.*, 2005, **59**, 200–205.
8 P. Matousek, M. Towrie, A. Stanley and A. W. Parker, *Appl. Spectrosc.*, 1999, **53**, 1485–1489.
9 M. D. Morris, P. Matousek, M. Towrie, A. W. Parker, A. E. Goodship and E. R. C. Draper, *J. Biomed. Opt.*, 2005, **10**, 014014.
10 P. Matousek, I. P. Clark, E. R. C. Draper, M. D. Morris, A. E. Goodship, N. Everall, M. Towrie, W. F. Finney and A. W. Parker, *Appl. Spectrosc.*, 2005, **59**, 393–400.
11 P. Matousek, M. D. Morris, N. Everall, I. P. Clark, M. Towrie, E. Draper, A. Goodship and A. W. Parker, *Appl. Spectrosc.*, 2005, **59**, 1485–1492.
12 E. Widjaja, C. Z. Li and M. Garland, *Organometallics*, 2002, **21**, 1991–1997.
13 J. Y. Ma and D. Ben-Amotz, *Appl. Spectrosc.*, 1997, **51**, 1845–1848.
14 M. V. Schulmerich, W. F. Finney, V. Popescu, M. D. Morris, T. M. Vanasse and S. A. Goldstein, Transcutaneous Raman spectroscopy of bone tissue using a non-confocal fiber optic array probe, in *Proceedings of SPIE 6093, Biomedical Vibrational Spectroscopy III: Advances in Research and Industry*, ed. A. Mahadevan-Jansen and W. H. Petrich, SPIE-INT Society Optical Engineering, 1000 20th St., PO Box 10, Bellingham, WA 98227-0010 USA, 2006, 60930O.
15 M. V. Schulmerich, W. F. Finney, R. A. Fredricks and M. D. Morris, *Appl. Spectrosc.*, 2006, **60**, 109–114.
16 P. Matousek, E. R. C. Draper, A. E. Goodship, I. P. Clark, K. L. Ronayne and A. W. Parker, *Appl. Spectrosc.*, 2006, **60**, 758–763.
17 P. Matousek, *Appl. Spectrosc.*, 2006, **60**, 1341–1347.
18 M. V. Schulmerich, K. A. Dooley, M. D. Morris, T. M. Vanasse and S. A. Goldstein, *J. Biomed. Opt.*, 2006, **11**, 060502.
19 M. V. Schulmerich, M. D. Morris, T. M. Vanasse and S. A. Goldstein, Transcutaneous Raman spectroscopy of bone global sampling and ring/disk fiber optic probes, in *Proceedings of SPIE 6430, Advanced Biomedical and Clinical Diagnostic Systems V*, ed. T. Vo-Dinh, W. S. Grundfest, D. A. Benaron, G. E. Cohn and R. Raghavachari, 2007, 643009.
20 P. Matousek and A. W. Parker, *Appl. Spectrosc.*, 2006, **60**, 1353–1357, and references therein.
21 P. Matousek and A. W. Parker, *J. Raman Spectrosc.*, 2007, **38**, 563–567.
22 E. R. C. Draper, M. D. Morris, N. P. Camacho, P. Matousek, M. Towrie, A. W. Parker and A. E. Goodship, *J. Bone Miner. Res.*, 2005, **20**, 1968–1972, and references therein.
23 B. R. McCreadie, M. D. Morris, T. Chen, D. S. Rao, W. F. Finney, E. Widjaja and S. A. Goldstein, *Bone*, 2006, **39**, 1190–1195.
24 A. Carden and M. D. Morris, *J. Biomed. Opt.*, 2000, **5**, 259–268.
25 R. Baker, P. Matousek, K. L. Ronayne, A. W. Parker, K. Rogers and N. Stone, *Analyst*, 2007, **132**, 48–53.
26 N. Stone, R. Baker, K. Rogers, A. W. Parker and P. Matousek, *Analyst*, 2007, DOI: 10.1039/b705029a, submitted.
27 P. Matousek and N. Stone, *J. Biomed. Opt.*, 2007, **12**, 024008, and references therein.
28 A. S. Haka, K. E. Shafer-Peltier, M. Fitzmaurice, J. Crowe, R. R. Dasari and M. S. Feld, *Cancer Res.*, 2002, **62**, 5375–5380.
29 C. Eliasson and P. Matousek, *Anal. Chem.*, 2007, **79**, 1696–1701.
30 C. Eliasson and P. Matousek, *Security screening: sugar in envelopes using transmission Raman spectroscopy*, Central Laser Facility, CCLRC Rutherford Appleton Laboratory, Didcot, UK, internal report, July 2006.
31 C. A. Lieber and A. Mahadevan-Jansen, *Appl. Spectrosc.*, 2003, **57**, 1363–1367.

